Distinct energy budgets for anthropogenic and natural changes during global warming hiatus

Shang-Ping Xie[1]*, Yu Kosaka[2] and Yuko M. Okumura[3]

The Earth's energy budget for the past four decades can now be closed[1], and it supports anthropogenic greenhouse forcing as the cause for climate warming. However, closure depends on invoking an unrealistically large increase in aerosol cooling[2] during the so-called global warming hiatus since the late 1990s (refs 3,4) that was due partly to tropical Pacific Ocean cooling[5-7]. The difficulty with this closure lies in the assumption that the same climate feedback applies to both anthropogenic warming and natural cooling. Here we analyse climate model simulations with and without anthropogenic increases in greenhouse gas concentrations, and show that top-of-the-atmosphere radiation and global mean surface temperature are much less tightly coupled for natural decadal variability than for the greenhouse-gas-induced response, implying distinct climate feedback between anthropogenic warming and natural variability. In addition, we identify a phase difference between top-of-the-atmosphere radiation and global mean surface temperature such that ocean heat uptake tends to slow down during the surface warming hiatus. This result deviates from existing energy theory but we find that it is broadly consistent with observations. Our study highlights the importance of developing metrics that distinguish anthropogenic change from natural variations to attribute climate variability and to estimate climate sensitivity from observations.

Atmospheric composition changes, caused by anthropogenic emissions of greenhouse gases and aerosols and by volcanic eruptions, perturb top-of-the-atmosphere (TOA) radiation flux. The resultant radiative forcing (F) has increased global mean surface temperature T (GMT) by 0.5 °C since 1950 (ref. 1). The warming modifies the TOA radiation by emitting more radiation into space. This climate feedback via TOA radiation (Q_C) is generally cast as

$$Q_C = -\lambda T \qquad (1)$$

an approximation that has been extensively validated in climate models for a forced response[8] (Supplementary Fig. 1). Here, λ is the climate feedback parameter (Supplementary Table 1), and downward TOA radiation Q is defined positive. Thus, the Earth's energy balance follows

$$dH/dt \approx Q = F - \lambda T \qquad (2)$$

where we have used the fact that 93% of the Earth's energy change is due to the change in ocean heat content H (OHC; ref. 1).

GMT increase has stalled for the past 15 years, often referred to as the global warming hiatus[5]. A downturn in the natural cycle of GMT, anchored by tropical Pacific cooling, is a leading hypothesis consistent with observed regional climate anomalies[6,9], although changes in the radiative forcing also contribute[10,11]. Here we examine the natural variability hypothesis. Generally, GMT change consists of the forced warming T_F and natural variability T_N: $T = T_F + T_N$. During the hiatus ($dT/dt = 0$), equation (1) predicts $dQ/dt = dF/dt$, much larger than the baseline of the forced response $dQ/dt = dF/dt - \lambda\, dT_F/dt$. Observations do not support this prediction of accelerated planetary energy uptake; OHC data do not show an acceleration in dH/dt (refs 12,13) and satellite data show little change in TOA radiation since 2000 (ref. 14). This is related to a problem noted earlier: the Earth energy budget cannot be closed based on equation (2) during the hiatus without invoking an unrealistic increase in aerosol forcing[3,4].

To resolve this discrepancy between energy theory (equation (2)) and observations, we investigate natural variability in climate models. We show that, unlike the forced response, TOA radiation and GMT are only weakly correlated in natural variability, invalidating equation (2) for decadal periods, when interference by natural variability is important. Our analysis offers a revision of equations (1) and (2) that is consistent with observations during the hiatus.

First we examine the relationship between GMT and net incoming TOA radiation (Q) in natural decadal variability, using the Coupled Model Intercomparison Project phase 5 (CMIP5) control simulations with radiative forcing fixed at pre-industrial levels. TOA radiation and GMT are highly correlated at a time lag for interannual variability due to El Niño/Southern Oscillation[13]. This result is in good agreement with TOA radiation observations (Supplementary Figs 2 and 3), lending confidence to the model simulations.

Here we focus on decadal and longer variability that is relevant to the hiatus. Unlike the forced response with a tight correlation (Supplementary Fig. 1), TOA radiation is only loosely related to GMT on decadal and longer timescales. Multi-model mean correlation peaks at −0.4, with Q lagging GMT by two years (Fig. 1a). On average, the peak regression of Q against GMT is smaller than the climate feedback parameter λ for a forced response by a factor of two (Fig. 1b). Equation (1) does not accurately describe this relationship. Rather, climate feedback on TOA radiation needs to be decomposed into distinct forced and natural variability components as

$$Q_C = -\lambda T_F - \lambda_N e^{-i\theta} T_N \qquad (3)$$

where T_N is a complex oscillatory function, and θ is the phase difference by which T_N leads outgoing TOA radiation ($-Q_N$). In CMIP5 pre-industrial simulations, θ varies between 45° and 90°,

[1]Scripps Institution of Oceanography, University of California San Diego, 9500 Gilman Drive MC 0206, La Jolla, California 92093, USA. [2]Research Center for Advanced Science and Technology, University of Tokyo, 4-6-1 Komaba, Meguro-ku, Tokyo 153-8904, Japan. [3]Institute for Geophysics, University of Texas at Austin, 10100 Burnet Road, Austin, Texas 78758, USA. *e-mail: sxie@ucsd.edu
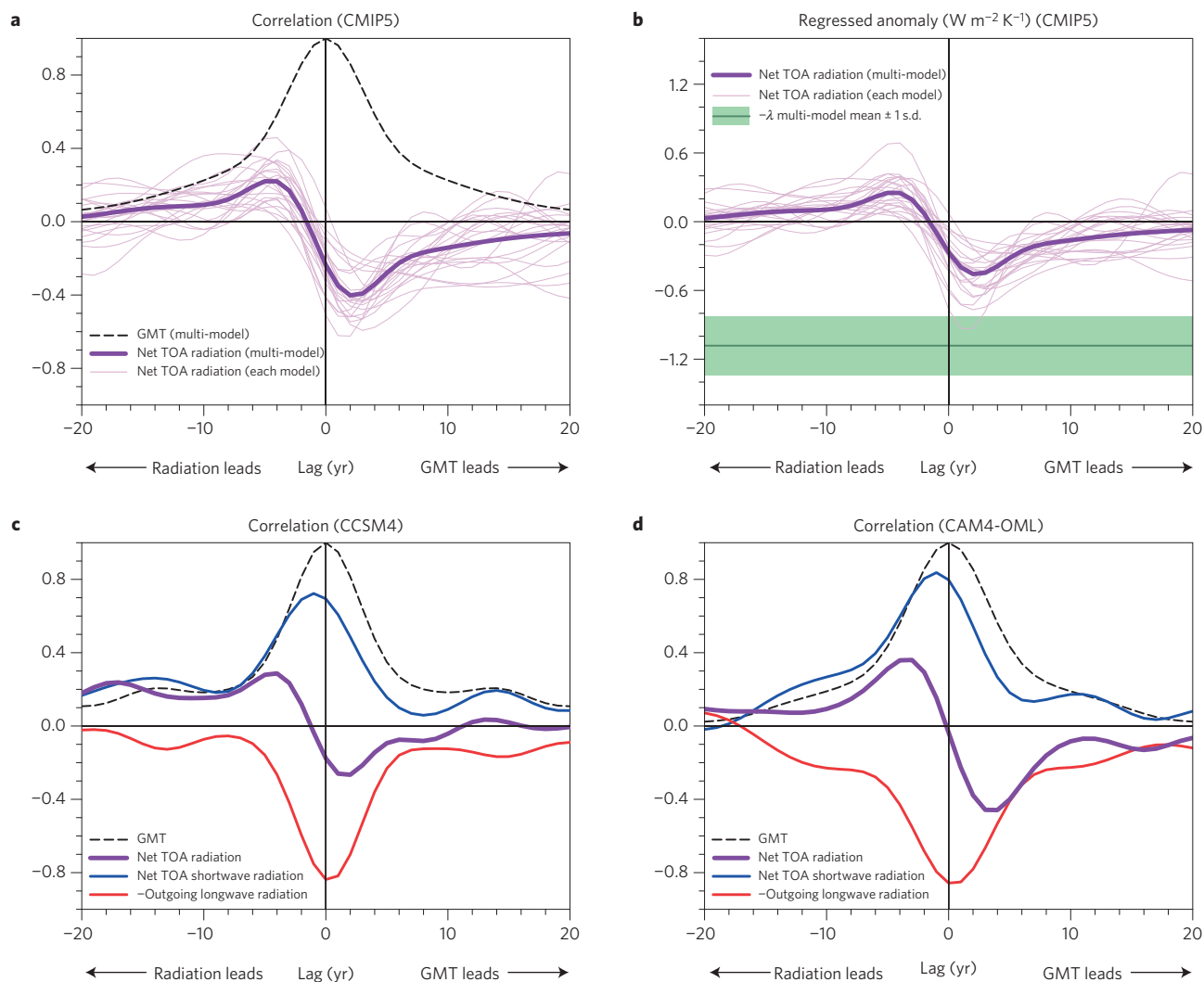
Figure 1 | Relationship between GMT and TOA radiation in natural decadal variability. a–d, Lagged correlation (**a,c,d**) and lagged regression (**b**) of net, net shortwave and outgoing longwave TOA radiation against GMT. Based on 10-year low-pass filtered pre-industrial simulations of CMIP5 (thin pale purple curves: individual models; thick purple curve: multi-model mean) (**a,b**), CCSM4 (**c**) and CAM4-OML (**d**). GMT autocorrelation is also shown in **a,c,d** as black dashed curves (multi-model mean in **a**). Multi-model mean and inter-model standard deviation of the forced climate feedback coefficient λ is superimposed on **b**. Positive lags indicate that GMT leads.

and $\lambda/\lambda_N \approx 2$ (Fig. 1b and Supplementary Fig. 2). We will show that the phase lag between Q and T allows a better comparison with TOA observations than traditional energy theory (equation (2)).

Climate feedback is distinct between the forced response and natural variability due to fundamental differences in the generation mechanism. Increases in well-mixed greenhouse gas concentrations perturb TOA radiation and induce surface warming everywhere[1]. Although the global energy balance is fundamental to anthropogenic warming, the low correlation between GMT and Q indicates that TOA radiation is not a major constraint on natural variability in GMT change. Instead, natural variability arises from atmospheric stochastic forcing and ocean–atmosphere feedback[15]. The resultant modes of variability feature preferred spatial patterns (for example, El Niño/Southern Oscillation and the Interdecadal Pacific Oscillation, IPO; refs 16,17), and global averages of surface temperature and TOA radiation are the residuals of large spatial variations of opposing signs (for example, between the tropical warming and North Pacific cooling in Fig. 2a). Remarkably, both the longwave and shortwave components of TOA radiation are highly correlated with GMT (Fig. 1c,d), but their sum (the net TOA flux) is not, because the two oppose each other. The high

longwave correlation at lag 0 is indicative of negative climate feedback, whereas the phase lead of shortwave variability suggests atmospheric stochastic forcing.

A popular energy theory argues that the surface warming hiatus happens because the subsurface ocean can store heat[13,18]. To evaluate whether subsurface ocean storage is essential for GMT variability, we compare a pair of coupled ocean–atmosphere simulations under a constant radiative forcing. The models share the same Community Atmosphere Model version 4 (CAM4), coupled to a full-depth dynamical ocean (Community Climate System Model version 4; CCSM4) and a motionless ocean mixed-layer (OML) model (CAM4-OML), respectively (Methods). With a dynamical ocean, CCSM4 features enhanced interannual variability including El Niño/Southern Oscillation compared to CAM4-OML, but GMT variance at timescales longer than 30 years is similar between the two models (Fig. 3a). The GMT spectrum is basically red in CAM4-OML.

The global distribution of decadal temperature variability regressed on GMT is also similar between the models, featuring an IPO-like pattern in the Pacific and a zonal band of increased temperature in high latitudes in each hemisphere (Fig. 2). The
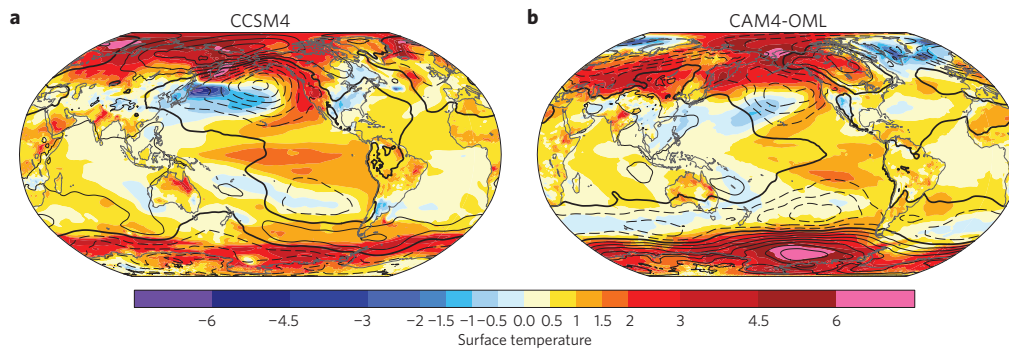
Figure 2 | Patterns of natural variability. a,b, Anomalies of surface temperature (shading, K K^{-1}) and sea-level pressure (contours from -7 to 7 in increments of 1 hPa K^{-1}; dashed for negative, thick solid for zero and thin solid for positive) regressed on unit GMT increase in CCSM4 (**a**) and CAM4-OML (**b**) simulations with constant radiative forcing. Ten-year low-pass filtered data are used. The anomaly pattern is overall similar between the two models, but in CCSM4 the surface temperature anomalies are locally intensified in the equatorial Pacific upwelling zone and along the Kuroshio Extension east of Japan due to ocean dynamic effects.
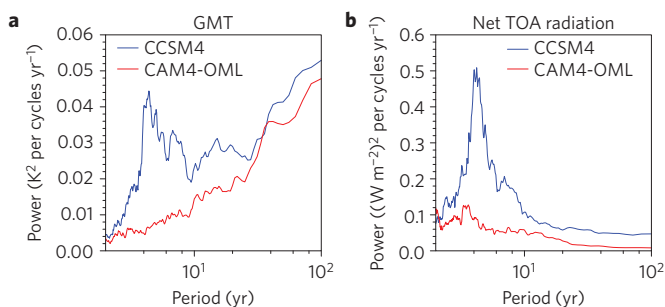

Figure 3 | Role of ocean dynamics in natural variability. a,b, Comparison of spectra for GMT (**a**) and net TOA radiation (**b**) between coupled models with a dynamic (CCSM4) and resting mixed-layer (CAM4-OML) ocean with constant radiative forcing. The largest differences are seen for periods shorter than ten years, which implies the importance of ocean dynamics for El Niño/Southern Oscillation.

IPO-like pattern common to both models supports the hypothesis that much of tropical decadal variability arises from thermodynamic ocean–atmosphere interactions[19,20]. This comparison suggests that subsurface ocean heat uptake is not essential for multi-decadal variability in GMT and decadal surface warming hiatus.

Consider a sinusoidal cycle of T_N with a period of $2(t_1-t_0)$, superimposed on a linear trend T_F forced by radiative forcing F (Fig. 4a,b). The natural variability T_N happens to have the downward phase that creates a warming hiatus ($dT/dt \approx 0$) during $t_0 < t < t_1$. We consider separately the radiative imbalance at TOA for the forced response ($Q_F = F - \lambda T_F$) and for natural variability (Q_N). Our revised energy view (equation (3)) calls for $Q_N < 0$ (green curve, assuming $\theta = 90°$ for illustration) and predicts a reduced TOA imbalance ($Q = Q_F + Q_N$; red curve) compared to the baseline of Q_F, whereas the traditional theory (equation (2)) predicts an accelerated increase in TOA imbalance during the hiatus ($Q_F - \lambda T_N$; brown curve).

We examine observations (Methods) to check the consistency of these distinct predictions. Neither TOA radiation nor OHC data support the traditional theory's prediction that net incoming TOA radiation increases at accelerated rates during the hiatus (Fig. 4d). TOA radiation data show a drop of 0.3 W m^{-2} from the late 1990s to mid-2000s (ref. 21), a change consistent with the revised energy view (the red curve in Fig. 4b). A caveat is that the data set consists of two separate records by different satellite instruments before and after 2000, calibrated with atmospheric model simulations[22]. Ocean observations suggest an increase in OHC since 1970, but the rate of increase (dH/dt) disagrees with TOA radiation in

interannual variability (Fig. 4c,d). Specifically, dH/dt shows a peak in 2002 whereas Clouds and Earth's Radiant Energy System (CERES) TOA radiation remains flat since 2000 (ref. 14). The disagreement could be due to the transition from expendable bathythermographs to Argo[23], insufficient sampling and unresolved instrumental biases as corroborated by the large spread among different OHC data sets[1].

An analysis of a global-warming simulation with Community Earth System Model version 1 (CESM1; Methods) confirms that TOA radiation drops below the baseline of the forced response during the hiatus (Fig. 4e,f), a result typical of other CMIP5 models[24,25]. The hiatus-related TOA radiation decrease is much weaker in magnitude in the model ten-event mean than in observations, but variability is large among 'hiatus' events. Although the early hiatus decrease in TOA radiation implied from observations[22] is broadly consistent with the revised energy view, data uncertainty and low decadal correlation between Q and GMT preclude a definitive test. This leaves open the possibility for changing radiative forcing to contribute to the recent hiatus[10,11].

Independent support for the revised energy view comes from the success of models in reproducing the observed decrease in planetary energy uptake[13] during 'interannual hiatus' events when the tropical Pacific transitions from El Niño to La Niña (between $t = 0$ and month 20 in Supplementary Fig. 3a). We note that the phase relationship between energy uptake and GMT is similar on interannual and decadal timescales (compare Supplementary Fig. 3a and Fig. 1a). The model skill on the interannual timescale lends some confidence to model results regarding the decadal hiatus.

In summary, we have shown that anthropogenic warming and natural variability are governed by distinct relationships between GMT and TOA radiation. Whereas a linear relationship is well established for the forced response, the correlation between GMT and TOA radiation is low and phase shifted for natural variability on decadal and longer timescales. We proposed a revised energy theory that distinguishes forced change and natural variability. Observations of TOA radiation and OHC during the recent warming hiatus are more compatible with the revised than traditional energy theory, although issues remain with quantitative validation because of data uncertainty and diversity in TOA radiation response among hiatus events. The weak climate feedback associated with natural GMT variability also explains why the traditional theory (equation (2)) successfully closed the energy budget over the past four decades when anthropogenic warming dominated[1], but had difficulty doing so during the current hiatus period[3,4] when forced warming and natural cooling are both important.

The TOA energy view is fundamental for understanding the forced change in GMT, but the energy constraint is weak on
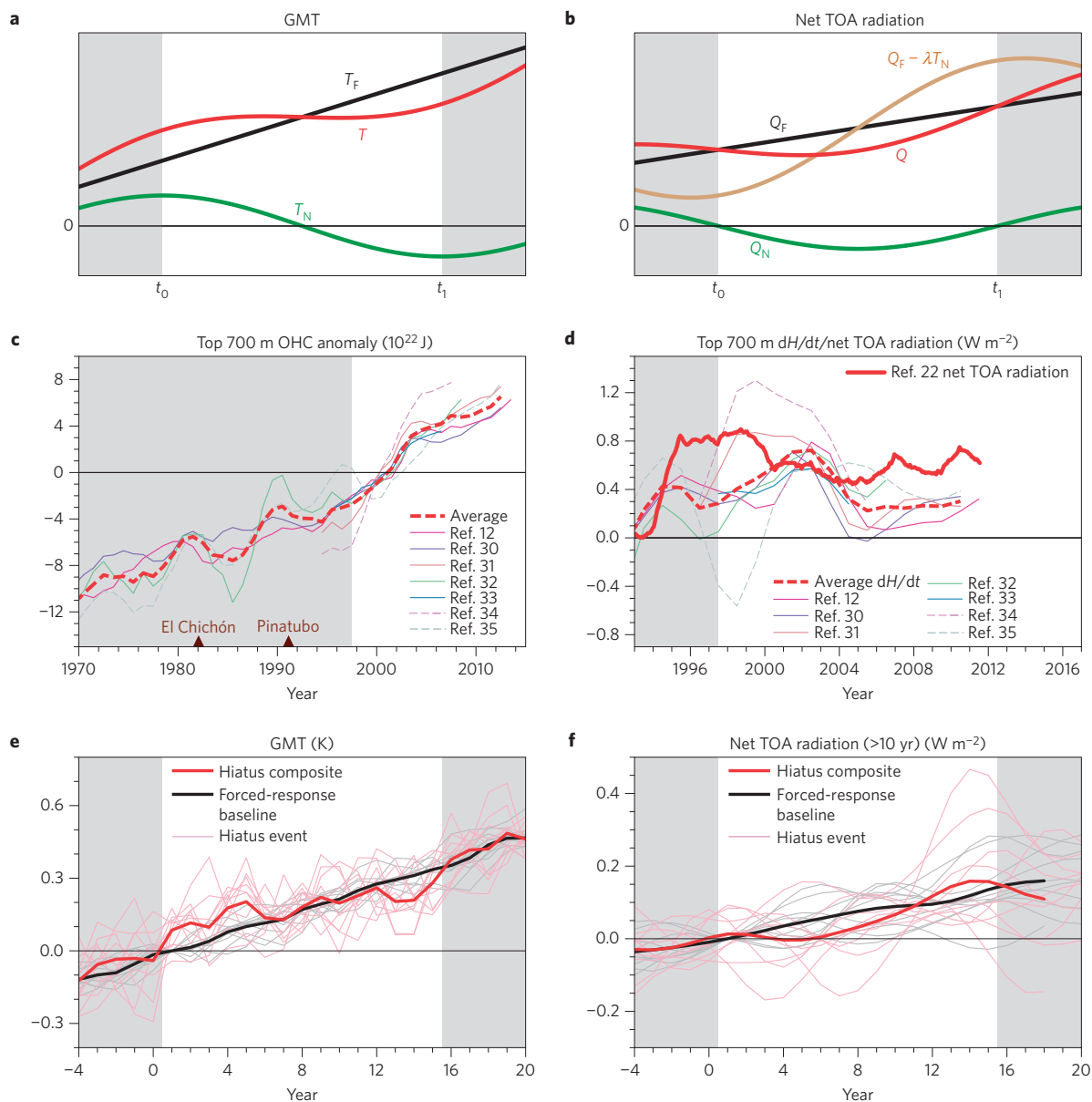
Figure 4 | GMT, TOA radiation and OHC during hiatus. a,b, Schematics of GMT (**a**) and TOA radiation (**b**). See main text for definitions. **c,d,** Observational estimates of OHC anomaly (**c**) and its tendency with reconstructed TOA radiation (**d**). **e,f,** GMT (**e**) and TOA radiation (**f**, ten-year low-pass filtered) for 'hiatus' events in a global-warming simulation. Thin pale and thick red curves represent individual hiatus events (years 1–15) and their average, respectively. Each thin pale black curve is the ten-member ensemble average for one of ten hiatus events, approximating the forced-response baseline. The thick black line is the average of the thin black lines. Ensemble means are adjusted to zero at year 1. TOA radiation deviation of hiatus events from the baseline is -0.0115 ± 0.0353 W m^{-2}.

natural variability, as is clear from comparison of energetics between simulations with a motionless OML and fully dynamic ocean (Methods). The climate feedback parameter λ_N depends on timescale[26], calling for caution in estimating climate sensitivity from observed natural variability.

Like TOA radiation, OHC integrated over the entire ocean depth is only weakly correlated with GMT (Supplementary Fig. 4). Ocean temperature variations in models show a complex vertical dipole structure, with a nodal line at 700 m on the decadal timescale[27]. Argo observations show a similar dipole, with a shallower node for interannual variability[28]. The ongoing effort to monitor ocean temperature change below 2 km will allow OHC to be integrated over a greater depth, with the benefit of suppressing natural variability while capturing more anthropogenic ocean warming. Sustained ocean observations are essential to study the coupled feedbacks

that generate natural variability, and to narrow uncertainties in estimating ocean heat uptake and radiative forcing[21,29]. As our study demonstrates, metrics that distinguish the anthropogenic warming and natural variability help advance physical understanding and improve the attribution of evolving climate anomalies.

References

1. IPCC *Climate Change 2013: The Physical Science Basis* (eds Stocker, T. F. *et al.*) 33–115 (Cambridge Univ. Press, 2013).
2. Murphy, D. M. Little net clear-sky radiative forcing from recent regional redistribution of aerosols. *Nature Geosci.* **6,** 258–262 (2013).
3. Murphy, D. M. *et al.* An observationally based energy balance for the Earth since 1950. *J. Geophys. Res.* **114,** D17107 (2009).

4. Church, J. A. *et al.* Revisiting the Earth's sea-level and energy budgets from 1961 to 2008. *Geophys. Res. Lett.* **38,** L18601 (2011).
5. Meehl, G. A., Arblaster, J. M., Fasullo, J. T., Hu, A. X. & Trenberth, K. E. Model-based evidence of deep-ocean heat uptake during surface-temperature hiatus periods. *Nature Clim. Change* **1,** 360–364 (2011).
6. Kosaka, Y. & Xie, S.-P. Recent global-warming hiatus tied to equatorial Pacific surface cooling. *Nature* **501,** 403–407 (2013).
7. England, M. H. *et al.* Recent intensification of wind-driven circulation in the Pacific and the ongoing warming hiatus. *Nature Clim. Change* **4,** 222–227 (2014).
8. Gregory, J. M. *et al.* A new method for diagnosing radiative forcing and climate sensitivity. *Geophys. Res. Lett.* **31,** L03205 (2004).
9. Watanabe, M. *et al.* Contribution of natural decadal variability to global warming acceleration and hiatus. *Nature Clim. Change* **4,** 893–897 (2014).
10. Schmidt, G. A., Shindell, D. T. & Tsigaridis, K. Reconciling warming trends. *Nature Geosci.* **7,** 158–160 (2014).
11. Santer, B. D. *et al.* Volcanic contribution to decadal changes in tropospheric temperature. *Nature Geosci.* **7,** 185–189 (2014).
12. Levitus, S. *et al.* World ocean heat content and thermosteric sea level change (0–2000 m), 1955–2010. *Geophys. Res. Lett.* **39,** L10603 (2012).
13. Trenberth, K. E., Fasullo, J. T. & Balmaseda, M. A. Earth's energy imbalance. *J. Clim.* **27,** 3129–3144 (2014).
14. Loeb, N. G. *et al.* Observed changes in top-of-the-atmosphere radiation and upper-ocean heating consistent within uncertainty. *Nature Geosci.* **5,** 110–113 (2012).
15. Liu, Z. Dynamics of interdecadal climate variability: A historical perspective. *J. Clim.* **25,** 1963–1995 (2012).
16. Zhang, Y., Wallace, J. M. & Battisti, D. S. ENSO-like interdecadal variability: 1900–93. *J. Clim.* **10,** 1004–1020 (1997).
17. Power, S., Casey, T., Folland, C., Colman, A. V. & Mehta, V. Inter-decadal modulation of the impact of ENSO on Australia. *Clim. Dynam.* **15,** 319–324 (1999).
18. Chen, X. & Tung, K.-K. Varying planetary heat sink led to global-warming slowdown and acceleration. *Science* **345,** 897–903 (2014).
19. Clement, A. C., DiNezio, P. & Deser, C. Rethinking the ocean's role in the Southern Oscillation. *J. Clim.* **24,** 4056–4072 (2011).
20. Okumura, Y. M. Origins of tropical Pacific decadal variability: Role of stochastic atmospheric forcing from the South Pacific. *J. Clim.* **26,** 9791–9796 (2013).
21. Smith, D. M. *et al.* Earth's energy imbalance since 1960 in observations and CMIP5 models. *Geophys. Res. Lett.* **42,** 1205–1213 (2015).
22. Allan, R. P. *et al.* Changes in global net radiative imbalance 1985–2012. *Geophys. Res. Lett.* **41,** 5588–5597 (2014).
23. Cheng, L. & Zhu, J. Artifacts in variations of ocean heat content induced by the observation system changes. *Geophys. Res. Lett.* **41,** 7276–7283 (2014).
24. Brown, P. T., Li, W., Li, L. & Ming, Y. Top-of-atmosphere radiative contribution to unforced decadal global temperature variability in climate models. *Geophys. Res. Lett.* **41,** 5175–5183 (2014).
25. Palmer, M. D. & McNeall, D. J. Internal variability of Earth's energy budget simulated by CMIP5 climate models. *Environ. Res. Lett.* **9,** 034016 (2014).
26. Dalton, M. D. & Shell, K. M. Comparison of short-term and long-term radiative feedbacks and variability in twentieth-century global climate model simulations. *J. Clim.* **26,** 10051–10070 (2013).
27. Katsman, C. A. & van Oldenborgh, G. J. Tracing the upper ocean's "missing heat". *Geophys. Res. Lett.* **38,** L14610 (2011).
28. Roemmich, D. *et al.* Unabated planetary warming and its ocean structure since 2006. *Nature Clim. Change* **5,** 240–245 (2015).
29. Hansen, J., Sato, M., Kharecha, P. & von Schuckmann, K. Earth's energy imbalance and implications. *Atmos. Chem. Phys.* **11,** 13421–13449 (2011).
30. Ishii, M. & Kimoto, M. Reevaluation of historical ocean heat content variations with time-varying XBT and MBT depth bias corrections. *J. Oceanogr.* **65,** 287–299 (2009).
31. Lyman, J. M. *et al.* Robust warming of the global upper ocean. *Nature* **465,** 334–337 (2010).
32. Palmer, M. D., Haines, K., Tett, S. F. B. & Ansell, T. J. Isolating the signal of ocean global warming. *Geophys. Res. Lett.* **34,** L23610 (2007).
33. Willis, J. K., Roemmich, D. & Cornuelle, B. Interannual variability in upper ocean heat content, temperature, and thermosteric expansion on global scales. *J. Geophys. Res.* **109,** C12036 (2004).
34. Gouretski, V. & Reseghetti, F. On depth and temperature biases in bathythermograph data: Development of a new correction scheme based on analysis of a global ocean database. *Deep-Sea Res. I* **57,** 812–833 (2010).
35. Domingues, C. M. *et al.* Improved estimates of upper-ocean warming and multi-decadal sea-level rise. *Nature* **453,** 1090–1093 (2008).

Author contributions

S.-P.X. conceived the study and wrote the paper. Y.K. and Y.M.O. contributed to the development of the idea and performed the analysis. All the authors discussed the results and commented on the manuscript.

Additional information

Supplementary information is available in the online version of the paper. Reprints and permissions information is available online at www.nature.com/reprints. Correspondence and requests for materials should be addressed to S.-P.X.

Competing financial interests

The authors declare no competing financial interests.

Methods

CMIP5 pre-industrial control simulations. Supplementary Table 1 lists CMIP5 control simulations used for Fig. 1a,b, and the forced climate feedback parameter λ derived from abrupt CO_2 quadrupling experiments[36]. We use 22 models with a single ensemble member for each model. In all models, the atmosphere and ocean are fully coupled, and radiative forcing (solar radiation, greenhouse gases, aerosols, ozone and land use) is fixed at pre-industrial levels. We have linearly detrended each model run to remove slow climate drift.

CCSM4 and CAM4-OML simulations. We analyse co-variability of GMT and TOA radiation in two long simulations: the last 500 years from a 1300-year run of CCSM4 (ref. 37), and a 500-year run of CAM4-OML (refs 19,20). The CCSM4 simulation is identical to that used as a CMIP5 pre-industrial control simulation. The two models share the same atmospheric component (CAM4). The ocean and atmosphere are fully coupled in CCSM4, whereas they are only thermodynamically coupled through surface heat flux in CAM4-OML. In CAM4-OML, sea surface temperature is computed from surface heat flux and a 'Q flux' that represents the effect of climatological ocean heat transport. The mixed-layer depth is based on the annual mean climatology, and Q flux based on the seasonally varying climatology of the CCSM4 control simulation. The CCSM4 and CAM4-OML also share the same land and sea ice models. Both CCSM4 and CAM4-OML simulations are conducted at nominal 1° horizontal resolution under pre-industrial radiative forcing. We have linearly detrended each run before analysis.

Comparison of energetics between CCSM4 and CAM4-OML. Natural GMT variability is not tied to TOA radiation (and by extension OHC) in a unique quantitative relationship as traditional energy theory assumes. Neither λ_N nor θ is a physical constant. Rather, both depend on subsurface ocean physics. First, the 30-year low-pass filtered variance of TOA radiation is five times smaller in CAM4-OML than CCSM4, in spite of comparable GMT variance (Fig. 3). Second, the GMT leads outgoing TOA radiation ($-Q$) by 90° in CAM4-OML whereas the phase lag θ is only 45° in CCSM4 (Fig. 1c,d). In CAM4-OML, by construction ($C_m\, dT/dt = Q$; C_m is OML heat capacity), the concurrent correlation between GMT and TOA radiation is exactly zero (Fig. 1d). The coupling with the subsurface ocean prevents TOA radiation from adjusting quickly to equilibrium, reducing the lead of the GMT over $-Q$ to about 45° in CCSM4 (Fig. 1c and Supplementary Fig. 2) with finite concurrent correlation.

An ensemble simulation of global warming. We use the ten-member ensemble simulations with a 1° version of CESM1-CAM5 obtained from Earth System Grid (https://www.earthsystemgrid.org) for Fig. 4e,f. Using the Representative Concentration Pathway (RCP) 4.5 radiative forcing for 2006–2080, the member simulations differ only in atmospheric initial conditions. Top ten hiatus events are selected as 15-year periods with the smallest linear trends of GMT from the 2006–2075 period. The forced response is evaluated as the ensemble mean for a given hiatus period.

OHC data sets. For Fig. 4c,d, we use observational data sets of top 700 m global OHC from refs. 12,30–35. For consistency with ref. 35, a three-year running average has been applied to the other data sets. The anomalies are relative to 1995–2006 averages. The average of the data sets is evaluated if at least four data sets are available. We evaluate OHC tendency with the centred difference of the annual mean values, and then apply a three-year running average. The top 700 m OHC does not fully capture the whole depth OHC but is relatively well correlated with GMT in CCSM4 (Supplementary Fig. 4). The coverage of ocean observations below 700 m deteriorates before the 2000s prior to the Argo era.

TOA radiation data. TOA radiation in Fig. 4d is based on a global data set that uses atmospheric model simulations to combine the Earth Radiation Budget Satellite (ERBE; 1985–1999), and the CERES (2000–2014) TOA observations from space[22]. A five-year running average has been applied for consistency with the OHC tendency.

Model-observational comparison of TOA radiation. The model co-variability between GMT and TOA radiation—net, and the shortwave and longwave components—on the interannual timescale is generally in agreement with observations (Supplementary Fig. 3). Specifically, the net TOA radiation response lags GMT by six months in both observations and models[38]. The peak regression is considerably larger than the climate feedback for forced change. The model correlations are smaller and decay faster with time lead/lag than in observations, possibly because of the longer records (≥300 years in CMIP5 versus ∼30 years in observations).

TOA radiation is available for January 1985–February 2014 for the combined ERBE-CERES record[22], and January 1979–February 2015 for European Centre for Medium-Range Weather Forecast (ECMWF) Interim Reanalysis (ERA-Interim; ref. 39), with three years after the Pinatubo eruption (June 1991–May 1994) excluded. The ERBE-CERES TOA radiation is used in combination with Hadley Centre-Climate Research Unit combined GMT version 4.3 (HadCRUT4; ref. 40). Each data set is deseasonalized with climatology for 1990–2008, excluding the three years after the Pinatubo eruption. The first and last 60 months of each record have been truncated for the band-pass filtering.

References

36. Forster, P. M. *et al.* Evaluating adjusted forcing and model spread for historical and future scenarios in the CMIP5 generation of climate models. *J. Geophys. Res.* **118,** 1139–1150 (2013).
37. Gent, P. R. *et al.* The community climate system model version 4. *J. Clim.* **24,** 4973–4991 (2011).
38. Spencer, R. W. & Braswell, W. D. On the misdiagnosis of surface temperature feedbacks from variations in Earth's radiant energy balance. *Remote Sensing* **3,** 1603–1613 (2011).
39. Dee, D. P. *et al.* The ERA-Interim reanalysis: Configuration and performance of the data assimilation system. *Q. J. R. Meteorol. Soc.* **137,** 553–597 (2011).
40. Morice, C. P., Kennedy, J. J., Rayner, N. A. & Jones, P. D. Quantifying uncertainties in regional and regional temperature change using an ensemble of observational estimates: The HadCRUT4 data set. *J. Geophys. Res.* **117,** D08101 (2012).